# Diagonal Material Matrices for Arbitrary Simplicial Meshes for Solving Poisson Problems With One Unknown Per Element

Fabrizio Bellina and Ruben Specogna

EMCLab, Polytechnic Department of Engineering and Architecture (DPIA), Università di Udine, 33100 Udine, Italy

**We present a technique to construct diagonal material matrices for *arbitrary* triangular and tetrahedral meshes and arbitrary scalar material parameters. The recipe is based on a novel dual complex called *folded Voronoï diagram*. The proposed matrices are tailored to enable the use of a complementary-dual formulation for Poisson problems featuring one unknown per element.**

***Index Terms*— Cell method (CM), consistency, diagonal discrete Hodge operators, diagonal mass matrices, diagonal material matrices, finite-integration technique (FIT), folded Voronoi diagram.**

## I. Introduction

CONSIDERING stationary current conduction as the paradigm Poisson problem in a connected region $\Omega$ of the 3-D Euclidean space, we want to solve

$$\begin{cases} \operatorname{curl} \mathbf{E} = \mathbf{0} \\ \operatorname{div} \mathbf{J} = 0 \\ \mathbf{J} = \sigma \mathbf{E} \end{cases} \tag{1}$$

where $\sigma$ is the electric conductivity; and $\mathbf{E}$ and $\mathbf{J}$ are the electric field and the current density vectors, respectively. The material parameter electric conductivity $\sigma$ is assumed to be a positive scalar value which is a piecewise uniform in each material region. The region boundary $\partial\Omega$ is partitioned into a set of $N^{\mathrm{i}}$ surfaces of perfect insulators $\partial\Omega_k^{\mathrm{i}}$, and a set of $N^{\mathrm{c}}+1$ disjoint equipotential surfaces (*electrodes*) of perfect conductors $\partial\Omega_k^{\mathrm{c}}$

$$\partial\Omega = \sum_{k=1}^{N^{\mathrm{i}}} \partial\Omega_k^{\mathrm{i}} + \sum_{k=0}^{N^{\mathrm{c}}} \partial\Omega_k^{\mathrm{c}}. \tag{2}$$

Electrode $\partial\Omega_0^{\mathrm{c}}$ is considered as reference for all voltages of the remaining electrodes, which are supposed to be assigned. $\mathbf{J}\cdot\mathbf{n}=0$ is set as boundary conditions (b.c.) on each $\partial\Omega_k^{\mathrm{i}}$, where $\mathbf{n}$ is the outward-oriented normal unit vector of $\partial\Omega$.

There are several formulations to numerically solve problems like (1). The scalar potential (SP) finite-element (FE) formulation based on nodal elements is the most commonly used. With this formulation, the unknowns are the SPs $\mathbf{V}$ sampled on the mesh nodes. The voltages $\mathbf{U} = -\mathbf{G}\mathbf{V}$ are associated with the mesh edges, where $\mathbf{G}$ is the edge-node incidence matrix. Finally, the array $\tilde{\mathbf{I}}$ of the currents through the mesh dual faces [1] can be defined.

However, there exist *complementary* formulations where currents $\mathbf{I}$ are associated with mesh faces, whereas the voltages $\tilde{\mathbf{U}}$ are evaluated on dual edges [2], [3]. The most commonly used complementary formulation is the one using a vector potential (VP) represented by the curl-conforming Nédélec edge elements [4] or other geometric basis functions [3].

There is a third class of complementary formulations that we call *complementary-dual*: they still use the SP $\tilde{\mathbf{V}}$, which is sampled on mesh dual nodes, one-to-one with mesh elements. A sound complementary-dual method is the mixed-hybrid (MH) FE formulation [5], which provides the same current density of VP formulation [5].

There is another complementary-dual formulation, much less explored in the literature, which features one unknown per element [7], [8]. The key ingredient to enable the use of this dual SP DSP formulation is the construction of a *diagonal mass matrix*, which is believed to be impossible for general simplicial meshes.

After an introduction to the DSP formulation in Section II, Section III shows a technique to build a diagonal matrix and its physical roots are apparent when exploiting an equivalence with electrical networks. Section IV presents some numerical results and then conclusions are drawn.

## II. DSP Formulation

The DSP formulation with one unknown per element is obtained by writing (1) in the geometric framework [1], [2], that is

$$\mathbf{C}^T\tilde{\mathbf{U}} = \mathbf{0} \tag{3}$$

$$\mathbf{D}\mathbf{I} = \mathbf{0} \tag{4}$$

$$\mathbf{I} = \tilde{\mathbf{S}}\tilde{\mathbf{U}} \tag{5}$$

where $\tilde{\mathbf{U}}$ is the voltage on dual edges, $\mathbf{I}$ is the current on mesh faces, $\mathbf{D}$ is the element-face incidence matrix, $\mathbf{C}$ is the face-edge incidence matrix, and $\tilde{\mathbf{S}}$ is the *dual conductance matrix* that maps $\tilde{\mathbf{U}}$ into $\mathbf{I}$. To implicitly satisfy (3), the SP $\tilde{\mathbf{V}}$ in the dual nodes is introduced through

$$\tilde{\mathbf{U}} = -\tilde{\mathbf{G}}\tilde{\mathbf{V}} + \tilde{\mathbf{U}}_s = -\mathbf{D}^T\tilde{\mathbf{V}} + \tilde{\mathbf{U}}_s \tag{6}$$

since $\tilde{\mathbf{G}} = \mathbf{D}^T$ and $\mathbf{C}^T\mathbf{D}^T = (\mathbf{D}\mathbf{C})^T = \mathbf{0}$ holds [2]. $\tilde{\mathbf{U}}_s$ is introduced to take into account the Dirichlet b.c., so that $\mathbf{C}^T\tilde{\mathbf{U}}_s = \mathbf{0}$ [5], [6]. By substituting (6) and (5) into (4), one gets

$$(\mathbf{D}\tilde{\mathbf{S}}\mathbf{D}^T)\tilde{\mathbf{V}} = \mathbf{D}\tilde{\mathbf{S}}\tilde{\mathbf{U}}_s \tag{7}$$

having the SP on dual nodes as unknowns.

Manuscript received August 16, 2019; revised October 31, 2019; accepted November 9, 2019. Date of current version January 20, 2020. Corresponding author: R. Specogna (e-mail: ruben.specogna@uniud.it).

Color versions of one or more of the figures in this article are available online at http://ieeexplore.ieee.org.

Digital Object Identifier 10.1109/TMAG.2019.2953299

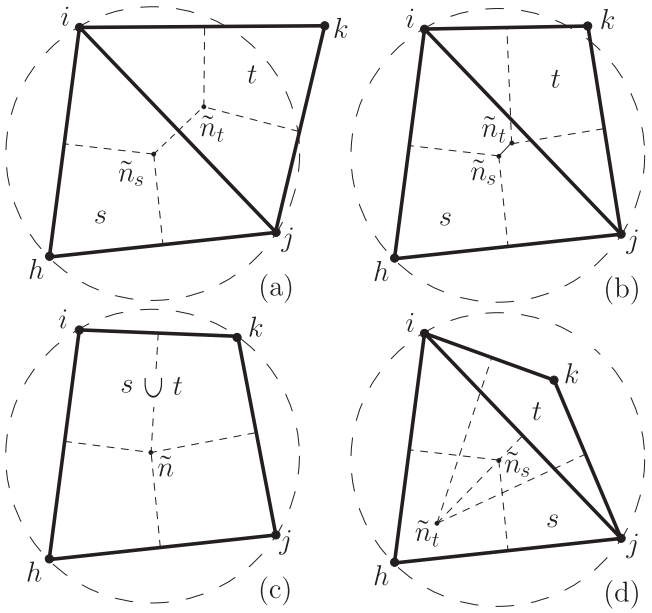


Fig. 1. (a) Two triangles $s$ and $t$ that satisfy the Delaunay condition and contain their circumcenters. (b) Two triangles $s$ and $t$ that satisfy the Delaunay condition but the circumcenter $\tilde{n}_t$ of $t$ lies outside $t$. (c) Degenerate case when four (or more) nodes lie on a circumference. This case is solved by perturbing the nodes or by creating a polygonal element. (d) Dual mesh of two triangles $s$ and $t$ that do not satisfy the Delaunay condition.

Matrix $\tilde{\mathbf{S}}$ may be computed as $\tilde{\mathbf{S}} = \mathbf{R}^{-1}$, where the *resistance mass matrix* $\mathbf{R}$ is the FE mass matrix obtained by using the div-conforming Raviart–Thomas face basis functions. Yet, the obtained matrix $\tilde{\mathbf{S}}$ is fully populated, hence not usable in practice. Another solution, reviewed in [6], is based on a geometric construction of $\tilde{\mathbf{S}}$ which, however, provides a matrix with such poor sparsity that the resulting formulation is again not competitive.

On the contrary, a diagonal conductance matrix $\tilde{\mathbf{S}}$ can be easily computed as described in Section III, which makes DSP formulation numerically efficient.

## III. Construction of Diagonal Material Matrices

### A. Survey on Diagonal Material Matrices

In the methods based on primal-dual interlocked meshes like the finite-integration technique (FIT) [9]; cell method (CM) [2], [10]; generalized finite differences [11]; discrete geometric approach (DGA) [3]; or discrete geometric methods (DGMs) [7], the commonly acknowledged condition to achieve diagonal matrices is that each dual node has to be placed in the *circumcenter* of the element to give rise to a pair of *orthogonal grids* [9], [10] [see Fig. 1(a)]. If the mesh is Delaunay (i.e., the circumcircle of every element contains no node in its interior), the dual interlocked mesh is called Voronoï diagram. The straight *dual edges* connect pairs of dual nodes relative to triangles sharing an edge or tetrahedra sharing a face. Since the Voronoï diagram is a partition of the input geometry into convex polygons or polyhedra, dual edges are always nonself-intersecting.

In literature, it is well known that it is hard to extend the construction of diagonal material matrices to arbitrary

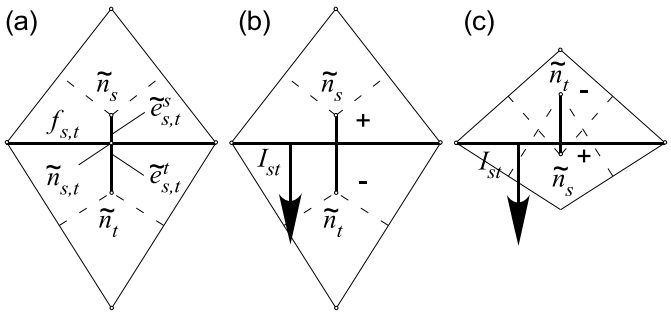


Fig. 2. (a) Geometric elements $s$ and $t$ involved in the conductance computation. (b) Positive dual edge length: the current is concordant with the potential difference. (c) Negative dual edge length: the current is discordant with the potential difference.

unstructured simplicial meshes. Many articles, in fact, including a recent account of the CM [2, p. 73], state that to compute diagonal material matrices *each simplex must contain its circumcenter* (see [7] and [12]–[15]). If this hypothesis holds, the SP is assigned to each dual node $\tilde{n}_s$ inside the simplex $s$ and the current $I_{s,t}$ to each primal face $f_{s,t}$ between two adjacent elements $s$ and $t$. With reference to Fig. 2(a), let $\tilde{n}_{s,t}$ be a new, temporary node corresponding to the intersection between the dual edge $\tilde{e}_{s,t}$ and the primal face $f_{s,t}$. It is assumed that the potential is piecewise linear along the edge $\tilde{e}_{s,t}$, and therefore, the electric-field component along the edge is constant inside each element, that is

$$E^s_{s,t} = \frac{\tilde{V}[\tilde{n}_s] - \tilde{V}[\tilde{n}_{s,t}]}{|\tilde{e}^s_{s,t}|}, \quad E^t_{s,t} = \frac{\tilde{V}[\tilde{n}_{s,t}] - \tilde{V}[\tilde{n}_t]}{|\tilde{e}^t_{s,t}|} \tag{8}$$

where $|\tilde{e}^s_{s,t}|$ and $|\tilde{e}^t_{s,t}|$ are the lengths of the dual edge parts inside the two elements. Since the dual nodes are located at the element's circumcentres, each dual edge is orthogonal to its corresponding primal face; hence, the current-density orthogonal component at the two sides of the primal face is computed as $J^s_{s,t} = \sigma_s E^s_{s,t}$, $J^t_{s,t} = \sigma_t E^t_{s,t}$, where $\sigma_s$, $\sigma_t$ are the electrical conductivities in the two adjacent elements. In the end, by enforcing the continuity of the current density normal components, the relation between the current in the primal face and the dual nodes potentials can be expressed as

$$I_{s,t} = (\tilde{V}_s - \tilde{V}_t)\frac{|f_{s,t}|}{\frac{|\tilde{e}^s_{s,t}|}{\sigma_s} + \frac{|\tilde{e}^t_{s,t}|}{\sigma_t}} = \tilde{S}_{s,t}(\tilde{V}_s - \tilde{V}_t). \tag{9}$$

$\tilde{S}_{s,t}$ can be viewed as the equivalent conductance between the two dual nodes $\tilde{n}_s$ and $\tilde{n}_t$.

However, in most practical problems, the circumcenter frequently lies outside the element [like in Fig. 1(b) or Fig. 1(d)]. In that case, the dual edge of the Delaunay–Voronoï pair does not intersect the associated face. Without claiming to be exhaustive, to circumvent this issue, the solutions proposed in literature comprise techniques that give up the diagonality of the material matrices [14], [15] or techniques that do not even ensure consistency [7], [12], [16], yielding to schemes whose solution is not exact even for uniform fields.

In [8], a recipe to construct diagonal, consistent, and positive definite material matrices has been proposed for arbitrary triangular and tetrahedral *boundary conforming Delaunay meshes*

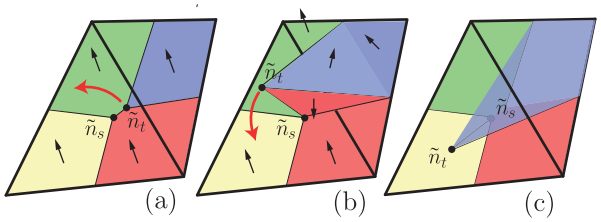


Fig. 3. (a) 3-D view of a standard 2-D Delaunay–Voronoï configuration. (b) Start to move dual node $\tilde{n}_t$ toward $\tilde{n}_s$. (c) Once one reaches the final position of $\tilde{n}_t$, the Voronoï diagram is folded.

for each piecewise uniform and isotropic material parameter. This method is able to fix the Delaunay configuration in Fig. 1(b) and the one in Fig. 1(c), but is still not able to deal with non-Delaunay meshes like the one shown in Fig. 1(d). The solution of [8] is formally the same as (9), but it introduces a novel *signed dual complex* in place of the classical Voronoï diagram. By signed dual complex, we mean that a *sign* is associated, in particular, to the lengths of the dual edge portions $|\tilde{e}^s_{s,t}|$ and $|\tilde{e}^t_{s,t}|$. The sign is computed as follows. The plane passing through face $f_{s,t}$ divides the space into two half-spaces. We consider the edge portion $\tilde{e}^s_{s,t}$ as always spanning from node $\tilde{n}_s$ to $f_{s,t}$ and we put a negative sign to $|\tilde{e}^s_{s,t}|$ if $\tilde{n}_s$ lies on a different half-space with respect to the node of $s$ not incident to $f_{s,t}$. The dual edge portion $|\tilde{e}^t_{s,t}|$ is defined in a similar way. The overall dual edge is constructed as the union of the two signed dual edge portions $|\tilde{e}^s_{s,t}|$ and $|\tilde{e}^t_{s,t}|$, so it joins nodes $\tilde{n}_s$ and $\tilde{n}_t$ but—differently from the standard Voronoï dual edge—it always intersects the associated face $f_{s,t}$ on $\tilde{n}_{s,t}$. In configurations like the one shown in Fig. 1(b), we could imagine that the signed dual edge is the result of folding of the dual edge on itself, but the Voronoï diagram is still a partition of the computational domain.

The remaining problem is that most mesh generators like GMSH or NETGEN do not provide boundary conforming Delaunay meshes, but even Delaunay meshes. Therefore, the problem of constructing a diagonal material matrix for arbitrary simplicial meshes is apparently still open for non-Delaunay configurations.

### B. Non-Delaunay Configurations

Let us analyze the problematic configuration where the mesh is not Delaunay [see Fig. 1(d)]. The first obstruction is that the dual of a non-Delaunay primal mesh is a Voronoï diagram which is not admissible given that it does not partition the computational domain.

However, in this article, we solve this first issue by defining a new dual complex that we call *folded Voronoï diagram*. In fact, as shown in Fig. 3, we can interpret the dual complex as the result of the folding of a standard Delaunay–Voronoï configuration. The areas with their signs remaining after folding are visible in Fig. 4. We remark that Fig. 4(a) and (c) exhibits a small triangle (represented in red) with a negative area. By summing up the signed area of all four dual faces, one obtains the computational domain as the union of the $r$ and $s$ triangles. This holds also for tetrahedral meshes by considering the portions of the dual volume with their appropriate sign.

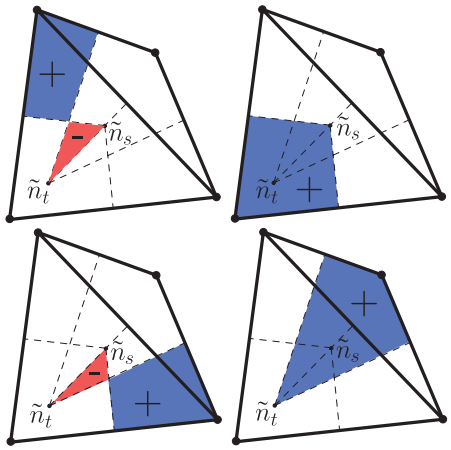


Fig. 4. Dual mesh of two triangles $s$ and $t$ does partition the computational domain if one considers the appropriate signs for area of the parts that make the dual faces.

The second issue is that with non-Delaunay simplicial meshes, some conductances produced by (9) become negative, which seems a nonphysical feature, since negative conductances give rise to currents with a verse apparently opposite to the electric field even in the presence of positive resistivity.

This article shows for the first time that there is a physical explanation also for negative conductances. A negative conductivity is the result of an electric port convention change obtained after folding. In the configuration of Fig. 2(b), the conductance is defined with the *passive sign convention*. On the contrary, on the non-Delaunay configuration of Fig. 2(c), the direction of the dual-edge is changed after folding and the *active sign convention* turns out to be used. Thus, the negative conductance is the result of the convention consistency.

A consequence of negative conductances is that the resulting matrix $\tilde{\mathbf{S}}$ is diagonal and consistent, albeit not positive definite. Indeed, nonpositive definite material matrices seem to be physically acceptable for the proposed application. In fact, we remark that the dissipated power is always positive once it is evaluated with the passive sign convention on all conductances. These material matrices have been extensively tested and so far we could not find any case in which the proposed approach fails.

### C. Analogy With Electric Circuits

It is well known that discrete formulations like that leading to (7) can be interpreted also in terms of equivalent lumped electric circuits, which can deal with both electrical and non-electrical phenomena (see [17]). To better understand the aspects related to a nonpositive definite matrix, the starting point is a dc network made of positive and negative conductances, in which each finite conductance $\tilde{S}_{s,t}$ is represented by a lumped component connected to nodes $\tilde{n}_s$ and $\tilde{n}_t$ and the boundary Dirichlet/Neumann boundary conditions are enforced through dc voltage, respectively, current generators.

The question is whether the solution of such a network, which is governed by the same $\tilde{\mathbf{S}}$ matrix as the DSP problem, exists and is unique. Instead of studying the dc network,

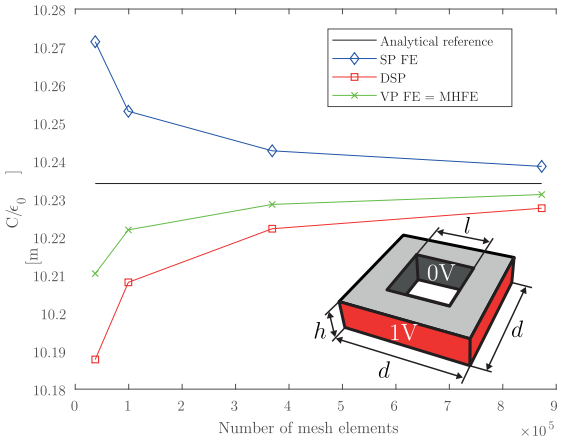


Fig. 5. Comparison of the convergence of the capacitance per unit of permittivity $C/\varepsilon_0$ with an increasing number of mesh elements of the proposed formulation with respect to two FE formulations.

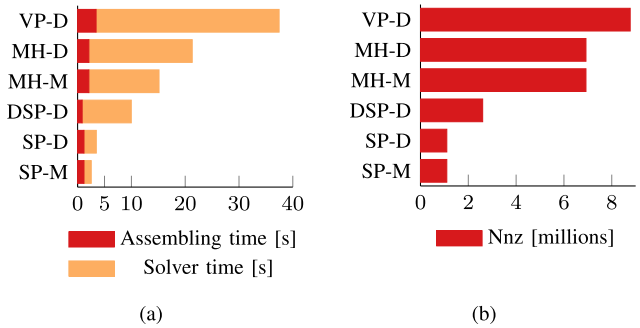


Fig. 6. (a) Simulation time on the finest mesh (about 870k tetrahedra, 146k nodes.) Flags M and D mean that algebraic multigrid solver (relative residual of $10^{-12}$) or Intel MKL PARDISO direct solver, respectively, has been used. (b) Number of nonzero entries (Nnz) of the sparse matrix.

taking inspiration from [17], the network is studied in sinusoidal regime with an arbitrary angular frequency $\omega$, and the positive and negative conductances $\tilde{S}_{s,t}$ are replaced, respectively, by inductances $L_{s,t} = 1/(\omega\tilde{S}_{s,t})$ and capacitances $C_{s,t} = -\tilde{S}_{s,t}/\omega$. The sufficient condition to have a unique solution in this purely reactive sinusoidal network, and therefore also in the dc network, is that no resonances occur. Note that if resonances exist, they exist for any $\omega$ because $L_{s,t}$ and $C_{s,t}$ are functions of $\omega$. The probability that the circuit exhibits a resonance at a fixed frequency $\omega$ is zero when arithmetic with arbitrary precision is used, because the resonances are countable and, therefore, they form a set of zero Lebesgue measures in $\mathbb{R}$. With floating-point arithmetic, the probability of a resonance is not zero anymore, but still extremely low.

## IV. Numerical Results and Conclusion

First, we verified that the proposed formulation fulfills the multi-material piecewise-uniform field patch test even when the material matrix is not positive definite. Among the further benchmarks considered, here there is the space to show the case of a square capacitor (Fig. 5) with $h = 1$, $d = 4$, and $l = 2$ m, for which the capacitance is known analytically ($C/\varepsilon_0 = 10.2340925$ m). The potential values on the internal and external electrodes are set, respectively, to 0 and 1 V, whereas zero normal field is imposed on the remainder of the capacitor surface. Fig. 5 shows how the capacitance computed by the proposed formulation converges to the analytical value when the number of tetrahedral mesh elements is increased. Even though the presented test case exhibits strong corner singularities in the solution, the proposed formulation shows an error which is symmetric with respect to the one of the SP FE formulations. As a comparison, the results provided by the SP FE formulation and those provided by the VP FE formulation VP or the algebraically equivalent MH FE formulation are also shown. The proposed DSP formulation turns out to be the fastest complementary formulation thanks to the excellent sparsity of the provided matrix (see Fig. 6). In the simulation on the finest mesh (about 870k tetrahedra, 146k nodes), 37.2% of circumcenters lie outside their elements and 2.2% faces exhibit a negative conductance. The exploitation of the proposed diagonal material matrices to other electromagnetics problems is an ongoing work.

## References

[1] A. Bossavit, "How weak is the 'weak solution' in finite element methods?" *IEEE Trans. Magn.*, vol. 34, no. 5, pp. 2429–2432, Sep. 1998.
[2] E. Tonti, *The Mathematical Structure of Classical and Relativistic Physics: A General Classification Diagram*. New York, NY, USA: Springer, 2013.
[3] R. Specogna, "Complementary geometric formulations for electrostatics," *Int. J. Numer. Methods Eng.*, vol. 86, no. 8, pp. 1041–1068, 2011.
[4] Z. Ren, "A 3D vector potential formulation using edge element for electrostatic field computation," *IEEE Trans. Magn.*, vol. 31, no. 3, pp. 1520–1523, May 1995.
[5] A. Bossavit, "Mixed-hybrid methods in magnetostatics: Complementarity in one stroke," *IEEE Trans. Magn.*, vol. 39, no. 3, pp. 1099–1102, May 2003.
[6] R. Specogna, "One stroke complementarity for Poisson-like problems," *IEEE Trans. Magn.*, vol. 51, no. 3, Mar. 2015, Art. no. 7401404.
[7] Z. Ren and X. Xu, "Dual discrete geometric methods in terms of scalar potential on unstructured mesh in electrostatics," *IEEE Trans. Magn.*, vol. 50, no. 2, Feb. 2014, Art. no. 7000704.
[8] R. Specogna, "Diagonal discrete Hodge operators for simplicial meshes using the signed dual complex," *IEEE Trans. Magn.*, vol. 51, no. 3, 2015, Art. no. 7400904.
[9] T. Weiland, "A discretization model for the solution of Maxwell's equations for six-component fields," *Electron. Commun.*, vol. 31, no. 3, pp. 116–120, 1977.
[10] E. Tonti, *On the Formal Structure of Physical Theories*. Rome, Italy: Italian National Research Council, 1975.
[11] A. Bossavit, "'Generalized finite differences' in computational electromagnetics," *Prog. Electromagn. Res.*, vol. 32, pp. 45–64, 2001.
[12] U. V. Rienen and T. Weiland, "Triangular discretization method for the evaluation of RF-fields in cylindrically symmetric cavities," *IEEE Trans. Magn.*, vol. MAG-21, no. 6, pp. 2317–2320, Nov. 1985.
[13] M. Marrone, "Computational aspects of cell method in electrodynamics," *Prog. Electromagn. Res.*, vol. 32, pp. 317–356, Dec. 2002.
[14] A. Canova, G. Gruosso, and M. Repetto, "3D electrostatic field solution with dual mesh," *Facta Univ.-Ser., Electron. Energetics*, vol. 15, no. 2, pp. 151–163, 2002.
[15] L. Bernard and L. Pichon, "Generalized finite difference scheme using mainly orthogonal and locally barycentric dual mesh for electromagnetic problems," *Eur. Phys. J.-Appl. Phys.*, vol. 52, no. 2, p. 23307, 2010.
[16] P. Alotto, A. De Cian, and G. Molinari, "A time-domain 3-D full-Maxwell solver based on the cell method," *IEEE Trans. Magn.*, vol. 42, no. 4, pp. 799–802, Apr. 2006.
[17] G. Kron, "Numerical solution of ordinary and partial differential equations by means of equivalent circuits," *J. Appl. Phys.*, vol. 16, no. 3, pp. 172–186, Apr. 1945.